Analytica Chimica Acta 930 (2016) 39–48

Contents lists available at ScienceDirect

Analytica Chimica Acta

journal homepage: www.elsevier.com/locate/aca

Mapping molecular adhesion sites inside SMIL coated capillaries using atomic force microscopy recognition imaging

Michael Leitner [a, 1], Lorenz G. Stock [b, c, 1], Lukas Traxler [a], Laurent Leclercq [d], Klaus Bonazza [e], Gernot Friedbacher [e], Hervé Cottet [d], Hanno Stutz [b, c], Andreas Ebner [a, *]

[a] Institute of Biophysics, Johannes Kepler University Linz, Gruberstrasse 40, 4020 Linz, Austria
[b] Division of Chemistry and Bioanalytics, Department of Molecular Biology, University Salzburg, Hellbrunnerstrasse 34, 5020 Salzburg, Austria
[c] Christian Doppler Laboratory for Innovative Tools for the Characterization of Biosimilars, University Salzburg, Hellbrunnerstrasse 34, 5020 Salzburg, Austria
[d] Institut des Biomolécules Max Mousseron (IBMM, UMR 5247, CNRS, Université de Montpellier, Ecole Nationale Supérieure de Chimie de Montpellier), Place Eugène Bataillon, CC 1706, 34095 Montpellier, France
[e] Institute of Chemical Technologies and Analytics, Vienna University of Technology, Getreidemarkt 9/164, 1060 Vienna, Austria

HIGHLIGHTS

- SMIL coating allows generation of homogeneous ultra-flat surfaces.
- Molecular electrostatic adhesion forces can be determined in the inner wall of CZE capillary with pico-Newton accuracy.
- Topographical images and simultaneously acquired adhesion maps yield morphological and chemical information at the nanoscale.

GRAPHICAL ABSTRACT

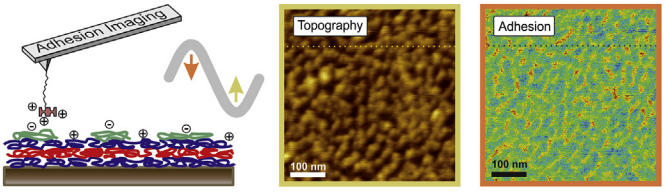

ARTICLE INFO

Article history:
Received 3 December 2015
Received in revised form
29 April 2016
Accepted 1 May 2016
Available online 4 May 2016

Keywords:
Recognition imaging
Adhesion forces
Capillary electrophoresis
Atomic force microscopy
SMIL coating

ABSTRACT

Capillary zone electrophoresis (CZE) is a powerful analytical technique for fast and efficient separation of different analytes ranging from small inorganic ions to large proteins. However electrophoretic resolution significantly depends on the coating of the inner capillary surface. High technical efforts like Successive Multiple Ionic Polymer Layer (SMIL) generation have been taken to develop stable coatings with switchable surface charges fulfilling the requirements needed for optimal separation. Although the performance can be easily proven in normalized test runs, characterization of the coating itself remains challenging. Atomic force microscopy (AFM) allows for topographical investigation of biological and analytical relevant surfaces with nanometer resolution and yields information about the surface roughness and homogeneity. Upgrading the scanning tip to a molecular biosensor by adhesive molecules (like partly inverted charged molecules) allows for performing topography and recognition imaging (TREC). As a result, simultaneously acquired sample topography and adhesion maps can be recorded. We optimized this technique for electrophoresis capillaries and investigated the charge distribution of differently composed and treated SMIL coatings. By using the positively charged protein avidin as a single molecule sensor, we compared these SMIL coatings with respect to negative charges, resulting in adhesion maps with nanometer resolution. The capability of TREC as a functional investigation technique at the nanoscale was successfully demonstrated.

* Corresponding author.
E-mail address: andreas.ebner@jku.at (A. Ebner).
[1] Authors contributed equally.

http://dx.doi.org/10.1016/j.aca.2016.05.002
0003-2670/

1. Introduction

Due to the high separation efficiency and electrophoretic resolution, capillary zone electrophoresis (CZE) represents an indispensable tool in bioanalysis. The electroosmotic flow (EOF) is an important parameter in CZE that modifies the apparent separation selectivity. The EOF is determined by the charge density at the inner capillary surface, the pH, and the ionic strength of the background electrolyte (BGE) [1]. However, protein adsorption onto the inner wall of fused-silica separation capillaries is an issue of concern in capillary electrophoresis impairing electrophoretic efficiency and resolution, signal intensity, and repeatability [2]. For macromolecules with inherent adhesion propensity, i.e. proteins, application of bare fused-silica capillaries requires operation at extreme pH values and/or BGEs of high ionic strengths to prevent adsorption events. This might represent unfavorable conditions if native protein conformation has to be maintained, Joule heating should be prevented or capillary electrophoresis-mass spectrometry (CE-MS) hyphenation is intended. Thus, different preventive means have been developed and optimized as reviewed elsewhere [3,4]. Strategies comprise dynamic capillary coating [5–7], physical polymer adhesion [8–12] and covalent coating [13,14]. High efforts have enhanced and are expected to further enhance the performance of capillaries for effective biomolecule separation. Successive Multiple Ionic Polymer Layer (SMIL) coating, introduced by Katayama et al. [15,16], is such a promising approach fulfilling the requirements of CZE. There, alternating layers of oppositely charged polymers are immobilized on bare fused-silica capillaries and microchips [17] by subsequent rinsing with cationic and anionic polymer solutions. SMIL coatings provide improved separation performance for peptides and proteins compared to uncoated capillaries with up to 685,000 theoretical plates [12,16] and stabilize the EOF and thus migration times. SMIL layer composition and preparation have been optimized and adopted to their respective target analytes [9,12,18] including biopharmaceuticals [19], recombinant allergens [12], model proteins [9,20,21], synthetic peptides [18], and (glyco) peptides [22,23], all using standard fused-silica capillaries with a circular cross-section.

Due to the chemical structure of the used polymers, relevant surface properties like roughness, and more important, the effective charge can be switched. Separations with these capillaries directly show their performance and thus give information on their usability. With an appropriately optimized coating protocol they provide durability from days to several weeks [12,20]. Nevertheless, a systematic quality proof is required to understand all analytical relevant processes sufficiently [24]. A first limitation is given by the accessibility of the inner capillary surface due to their small inner diameter in the range of 100 μm or less. Furthermore, the inner capillary coating can be significantly altered by preparation techniques including drying or any mechanical treatment resulting in measurement artefacts [24]. Finally, a lateral and vertical resolution in the nanometer range is required. Scanning electron microscopy as well as X-ray photoelectron spectroscopy fail regarding their ability to investigate adhesive properties and the requirement to measure topography in liquid environment. Atomic force microscopy (AFM) imaging has established as the best suited technique, since it allows determining the surface roughness with nanometer accuracy under buffered conditions. AFM imaging has been successfully applied to measure the morphology directly within the capillary itself [25–28] or on flat substrates mimicking the inner surface of electrophoresis capillaries [29–32]. These studies gained information about the topography of bare fused-silica surfaces as well as about different coatings used in capillary electrophoresis. Furthermore, scratching experiments were used to determine the thickness of the coatings. Beneath these structural investigations, attempts to explore their adhesive behavior have been started. Haselberg et al. [29] observed a 3 nm height increase of a polybrene − dextran sulfate (DS) − polybrene coating after incubation with cytochrome c indicating strong electrostatic binding. To gain further information on the electrostatic adhesion properties especially on the distribution of charges at the terminal coating on the inner capillary wall a new technical approach is needed. Topography and recognition imaging (TREC) fulfills these requirements. In TREC measurements the scanning tip is upgraded to a (monomolecular) biosensor. This technique has been applied to specifically localize different biomolecules like biotin [33,34], or proteins (e.g. cellular membrane receptors) on different surfaces ranging from isolated molecules over artificial [35] and native membranes [36] to cellular surfaces (for a review see Ref. [37] or [38]). In all these measurements, specific binding partners (e.g. antigen–antibody) have been used. Within this study, we performed TREC measurements to gain a map of charge distributions on the bulk exposed surface of a SMIL coated capillary while simultaneously scanning the sample topography.

2. Materials and methods

2.1. Chemicals

If not stated otherwise all chemicals were used at highest purity available. 3-Aminopropyltriethoxysilane (APTES), chloroform, citric acid, buffer salts, ethanol, formic acid (98–100%; puriss.), triethylamine (TEA), sodium chloride (≥99.5%), avidin, streptavidin, poly(diallyldimethylammoniumchloride) (PDADMAC) (20% wt in water; M_r 400,000–500,000), dextran sulfate sodium salt (M_r > 500,000) from *Leuconostoc* spp., and di-sodium hydrogen phosphate dihydrate (min. 99.5%) were purchased from Sigma-Aldrich (Vienna, Austria). *Ortho*-phosphoric acid (w ≥ 85.0%) was obtained from Merck (Darmstadt, Germany). Sodium hydroxide (standard volumetric solution 1 M) and Parafilm™ were from AppliChem (VWR International GmbH, Vienna, Austria). Ammonium bicarbonate (specified as eluent additive for LC-MS) was purchased from Fluka (Buchs, Switzerland). The commercially available linker NHS-PEG(18)-Acetal [39] was purchased from Prof. Gruber (JKU Linz, Austria). Poly(acrylamide-co2-acrylamido-2-methyl-1-propansulfonate) with a molar ratio of charged monomers of 55% (55% PAMAMPS) was synthetized by radical polymerization as described elsewhere [40]. The molar mass of the 55% PAMAMPS determined by size exclusion chromatography is ~640,000 g/mol (polydispersity index = 2.8). The hydrodynamic diameter of DS was 90–100 nm whereas the hydrodynamic diameter for 55% PAMAMPS was determined to be ~40–42 nm by Taylor dispersion analysis (TDA) [41] in storage buffer. Structures of the polyelectrolytes (PEs) applied in SMIL coating are provided in Fig. 1A (DS), B (55% PAMAMPS), and C (PDADMAC). Recombinant major pollen allergen of birch (*Betula verrucosa*), specified as isoform Bet v 1a, was nitrated in-lab with peroxynitrite [42] and used for the comparison of CZE-performance and the mobility of the EOF (μ_{EOF}) of different SMIL-coated capillaries (Section 3.1). Ultrapure water with 18 MΩ cm resistivity was used for all preparations (MilliQ grade, Millipore, Austria). Argon 5.0 and nitrogen 5.0 gas were purchased from Linde (Vienna, Austria).

2.2. Capillary SMIL coating

Circular fused-silica capillaries with 50 μm inner diameter (i.d.) and 360 μm outer diameter (o.d.) were used for CZE measurements. For AFM measurements square shaped fused-silica capillaries with 100 μm i.d. and 360 μm o.d. were used. Both capillary types were purchased from Polymicro Technologies (Phoenix, AZ, USA). The

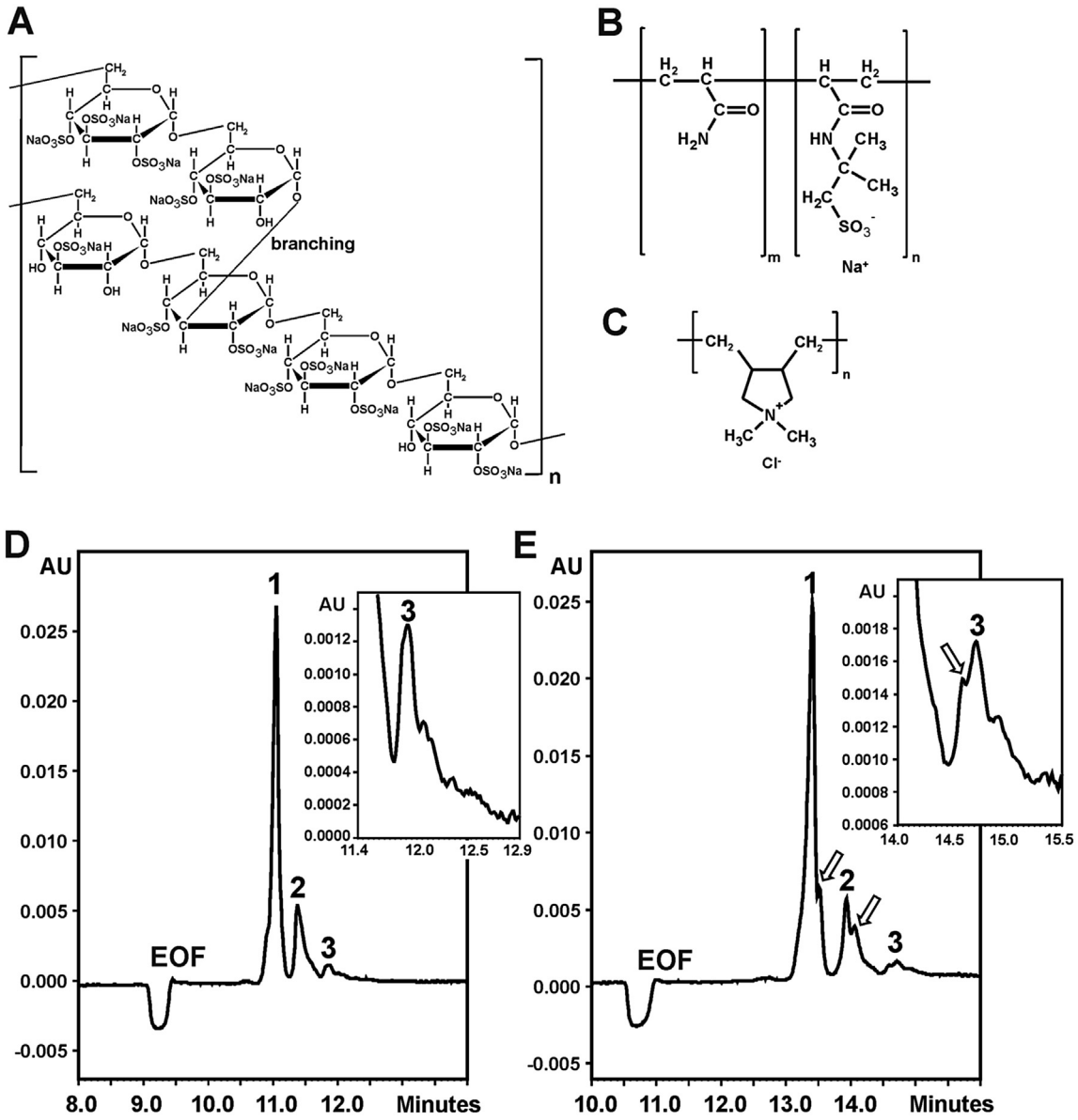

Fig. 1. Structures of PE used for the preparation of the respective SMIL coating. (A) DS with branched structure. (B) Structure of 55% PAMAMPS. The annotation as 55% PAMAMPS is related to the following ratio: n/(n + m) = 55%. (C) PDADMAC. (A) and (B) represent polyanionic PEs and constitute the terminal layer in the respective SMIL coating, whereas (C) is a polycationic polymer. (D, E) Comparison of CZE performance and EOF for two SMIL-coated circular capillaries with identical PE basal layer structure (PDADMAC-DS-PDADMAC) and a different terminal layer, (D) DS, (E) 55% PAMAMPS. Inserts depict details. Arrows indicate minor fractions resolved due to improved resolution in SMIL-55% PAMAMPS. Capillaries: 50 μm i.d., 360 μm o.d., effective capillary length (L_D) 39.7 cm, total capillary length (L_T) 50.1 cm. BGE: 50 mmol L^{-1} NH_4HCO_3, pH 6.50, 8.0 KV; 30.0 °C. 210 nm. Sample: nitrated Bet v 1a. Peaks: 1: non-modified Bet v 1a; 2, 3 and minor peaks: nitrated Bet v 1a variants.

total capillary length of the square capillary was 82.6 cm. The described coating procedure was based on a previous protocol [12] and applied for coating both circular and square capillaries, except that the voltage conditioning had to be adjusted to the different i.d. Since the finally applied coating protocol included some amendments the SMIL coating procedure is described in the following paragraphs. The polyelectrolytes (PE) used for SMIL coating were dissolved in an aqueous solution containing 80 mmol L^{-1} NaCl and 20 mmol L^{-1} di-sodium hydrogen phosphate buffer adjusted to pH 7.00 with *ortho*-phosphoric acid, i.e. deposition solution (DPS). PE coating solutions were prepared with the following concentrations: 0.20% (v/v) PDADMAC, 0.20% (w/v) DS, and 0.20% (w/v) 55% PAMAMPS. PDADMAC and DS were dissolved in DPS at least 1.5 h before the coating procedure was started. 55% PAMAMPS was dissolved the day before coating to allow for chain relaxation of the PE. Prior to their application in capillary coating all PE solutions were filtered through non-sterile 0.45 μm filters from Sartorius (Vienna, Austria).

Square capillaries were prepared in the Agilent 7100 Capillary Electrophoresis System (Agilent Technologies, Waldbronn, Germany) while the P/ACE™ MDQ system (Beckman Coulter, Fullerton, CA, USA) was used for circular capillaries. The fused-silica capillaries were conditioned at 35.0 °C by rinsing with 1.0 mol L^{-1} NaOH (30.0 min), ultrapure water (5.0 min) and finally with the conditioning solution (100 mmol L^{-1} di-sodium hydrogen phosphate buffer adjusted to pH 6.50 with *ortho*-phosphoric acid; for 3.0 min), all at 93 kPa. Each PE layer was attached according to the following protocol [12] that was slightly modified. Briefly, the capillary was

flushed at room temperature outside the CE system by means of a syringe pump from ColeParmer Instrument Company (Vernon Hills, IL, USA) with a flowrate of 1.1 mL h^{-1} using a 1 mL syringe. Capillary rinsing with PE deposition solutions was done with the external syringe, respectively, to prevent contamination of the CE system and carryover effects. A PEEK-capillary of appropriate dimensions was used to assure tight connection between the capillary and the syringe. The PEEK-capillary was additionally sealed with Parafilm to prevent leaks.

The respective PE-solution was flushed through the capillary for 12.0 min followed by rinsing with conditioning buffer for 10.0 min. Afterwards the capillary was inserted in the CE system (at 30.0 °C) and flushed (93 kPa) with conditioning buffer for 3.0 min followed by application of 6.0 kV (10.0 min, with 0.17 min ramp time) with both capillary ends immersed in conditioning buffer. In the circular capillary 10.0 kV were applied to ensure corresponding power generation. After the voltage application the coating was allowed to rest for 10.0 min with both capillary ends placed in conditioning buffer. All addressed steps including the voltage conditioning and resting were performed during the deposition of each individual PE layer. Polycationic and polyanionic PE layers were attached in turn. The provided final SMIL stratification was PDADMAC-DS-PDADMAC-55% PAMAMPS or PDADMAC-DS-PDADMAC-DS, respectively.

After completion of the four PE layers, the SMIL capillary was flushed with BGE, i.e. 50 mmol L^{-1} di-sodium hydrogen phosphate buffer (pH 6.50, adjusted with *ortho*-phosphoric acid), for 20.0 min with subsequent application of 10.0 kV (with 0.17 min ramp time) for 30.0 min. The SMIL capillary was then rinsed with BGE for 5.0 min and a second voltage application (10.0 kV; 0.17 min ramp time) was done for 30.0 min. Finally, the capillary was flushed with storage buffer (200 mmol L^{-1} di-sodium hydrogen phosphate buffer, pH 6.50 adjusted with *ortho*-phosphoric acid) and stored with its ends dipped in storage buffer for 85–90 h prior to its further use.

After the surface characterization by AFM, the SMIL coating with 55% PAMAMPS as terminal layer was subjected to two rinsing steps with 0.050 mol L^{-1} NaOH (93 kPa, 5.0 min, respectively). Rinsing steps with NaOH were intermitted by rinsing with BGE (50 mmol L^{-1} di-sodium hydrogen phosphate buffer, pH 6.50, 93 kPa, for in total 30.0 min) and voltage application (9.0 kV, 0.17 min ramp, for in total 230.0 min) in BGE. After the second NaOH rinsing the capillary was flushed (5.0 min, 93 kPa) with conditioning buffer (100 mmol L^{-1} di-sodium hydrogen phosphate buffer, pH 6.50). Characterization of the capillary surface by AFM was done after the second rinsing step with NaOH. The application of NaOH rinsing served to investigate the influence on the SMIL surface since this is a frequent tool in capillary electrophoresis to detach adsorbed proteins from capillary surfaces.

2.3. Capillary electrophoresis

CZE separations with SMIL coated circular capillaries were performed with a Beckman Coulter P/ACE™ MDQ System (Fullerton, CA, USA) including a photodiode array detector. System control and data treatment were done with Karat 32 software, version 5.0. 50 mmol L^{-1} ammonium bicarbonate adjusted to pH 6.50 with formic acid was used as BGE to separate the model allergen. The volatile BGE was selected since it offers the option for subsequent hyphenation to mass spectrometry. Samples were injected hydrodynamically with 3.45 kPa for 10.0 s. CZE separations were done with +8.0 kV (cathode at detector side) at 30.0 °C. Between runs, capillaries were rinsed with the volatile BGE (100 kPa) for 5.0 min. Detection was at 210 mn.

2.4. AFM imaging

All AFM measurements have been performed on a Pico Plus 5500 AFM equipped with a MACMode™ controller and a TREC™ box (all from Agilent Technologies, Santa Clara, CA, USA). MSCT cantilevers (Bruker AFM Probes, Karlsruhe, Germany) have been used for imaging and molecular recognition force spectroscopy. For all TREC adhesion measurements Type VII MACLevers (Keysight Technologies, Santa Rosa, USA) were used. All measurements were performed under buffered conditions using storage buffer.

2.5. AFM tip chemistry

Coupling of single avidin molecules to the outer tip apex of MSCT and MAC cantilever was performed in close analogy to previously published protocols [39,43]. In a nutshell: Commercially available bare MSCT cantilevers were treated in a plasma cleaner (4.0 min, 30 W) and cleaned by incubation in chloroform (3 × 5.0 min) and ethanol (3 × 5.0 min) and dried in a gentle stream of nitrogen gas. Amino-functionalization of the tips was performed by gas phase deposition of APTES [44]. For this the cleaned cantilevers were placed into a 5 L desiccator and two chambers filled with 60 μL APTES and 20 μL TEA, respectively, were placed into the desiccator filled with argon gas. Both reactants were removed after a reaction time of 2.0 h and the desiccator was extensively rinsed with argon to remove unbound chemicals. To ensure a stable APTES coating, the tips were allowed to remain in the desiccator for 48.0 h. As a next step the cantilevers were immersed for 120 min in a 500 μL chloroform solution containing 1.0 mg NHS-PEG(18)-Acetal [39] linker and 0.50% (w/v) TEA as catalyst, followed by washing in chloroform (3×) and drying in a gentle stream of nitrogen gas. After de-protecting the acetal group (1.0% (v/v) citric acid for 10.0 min) resulting in aldehyde residues and washing in water (3×), the tips were placed in a solution of avidin (or streptavidin) (0.20 mg mL^{-1}) in PBS containing 40 mmol L^{-1} freshly prepared $NaCNBH_3$ for 120 min. To destroy remaining unreacted aldehydes ethanolamine (yielding a final concentration of ~100 mmol L^{-1}) was added after 120 min. After washing in PBS (3 × 5.0 min) the avidin (or streptavidin) functionalized tips were ready for sensing experiments and either used immediately or stored for up to 2 day at 4 °C in PBS.

2.6. Molecular recognition force spectroscopy

For Molecular Recognition Force Spectroscopy (MRFS) measurements MSCT probes were functionalized as described in Section 2.5. Avidin was coupled as sensing protein, whereby for control experiments the same protocol was applied to couple streptavidin. The functional avidin or streptavidin tip was prepared freshly before use and always kept in PBS to avoid denaturation. For MRFS experiments SMIL coating was either prepared (i) on the outer capillary wall (55% PAMAMPS) or (ii) inside the capillary (DS). For the first case (i), the coating protocol for inner wall coating was adopted. Briefly, the protective polyimide was thermally removed and the outer capillary surface was conditioned by dipping into the respective solutions. SMIL coating was done by dipping the capillary into the coating solutions instead of rinsing (Section 2.2) and voltage application was not performed. The coated capillary part was attached to the surface by pressing on a Parafilm stripe attached in the liquid cell which was covered with storage buffer. The functionalized cantilever was approached to the middle of the capillary and MRFS was started immediately after approaching. The pulling velocity was set to 600 nm s^{-1} for all measurements that were performed in a 300 nm z-range, respectively. The position of the tip was changed after every 250 curves to avoid position dependent artefacts. At least 3 independent datasets with

1000–2000 force distance cycles (FDCs) each were performed to gain sufficient statistics. The spring constant of the used cantilever was determined using the thermal noise method [45]. For each FDC showing interaction, unbinding length, unbinding force, and the spring constant in the moment of rupture were determined. Statistical analysis as described previously [46] yielded the most probable unbinding force and length at given conditions. The overall probability was calculated by dividing the number of FDCs exhibiting a binding event by the total number of FDCs. Specificity proof experiments were performed by exchanging an avidin for a streptavidin functionalized tip and by using poly(ethylenglycol) (PEG) functionalized tips without any coupled protein at the very same capillary.

2.7. Topography and recognition imaging

The protective polyimide layer of the capillary of interest was peeled off the glass body and pressed under buffer on a Parafilm stripe mounted at the AFM liquid cell surface to ensure tight attachment. A scalpel was used to split the capillary more or less parallel to the long axis or alternatively cut normal to the capillary axis. Although it needs some training, the success rate to orient the scalpel split along the dimension of the rectangular bore is very high. An optical microscope was used to check the geometry of the ruptured area. After opening the capillary the AFM liquid cell was oriented in a way that the direction of the cantilever was exactly parallel to the capillary. Under optical control the cantilever was either positioned above the opened area or (via a micro manipulation stage) moved inside the capillary opening. By careful positioning using the x, y- and z-stage of the AFM equipment we were able to place the cantilever into the inner part of the capillary. It has to be mentioned that this is the most critical step of the whole procedure since any contact of the (functionalized) AFM tip may cause mechanical or chemical damage of the sensor.

A frequency plot (i.e. a measurement of the amplitude as a function of the frequency) was performed to determine the resonance frequency of the cantilever. The excitation frequency for the topography and recognition measurements was set 500 Hz below this frequency. The cantilever was approached until the sensing tip got into contact with the inner capillary surface. All TREC measurements were performed under buffered conditions at 1.0 Hz line frequency. The amplitude was set to ~8 nm to ensure upper damping of the oscillation in case of molecular (avidin – SMIL) interaction. Image processing was performed by Gwyddion (Version 2.41) using line and area flattening. Surface roughness was calculated by Gwyddion using root mean square (RMS) determination.

3. Results

SMIL represents a quasi-permanent physically adhered coating with an improved capillary-to-capillary reproducibility and a considerably more facile preparation than laborious multi-step covalent coatings [16]. Additionally, SMIL possesses higher durability - particularly with accordingly optimized protocols [12] - than dynamic coatings and thus compatibility with CE-ESI-MS [19]. Due to the overcharging of SMIL, a strong EOF is generated with low pH-dependence thus improving the separation repeatability. Consistently, high flow rates driven by the electric field are assured even at pH values where they are otherwise not generated. This accelerates the separation and promotes a stable electrospray particularly in sheathless MS interfaces. However, closely related protein variants often require EOF-tuning to exploit subtle differences in their effective electrophoretic mobilities efficiently. Therefore, polyionic polymers with reduced charge density to allow for both a lower but still repeatable EOF and stable anchoring to the subjacent polymer layer are aimed. 55% PAMAMPS represents a candidate polymer that has recently been tested successfully in different charge states for this purpose with peptides [40]. Results presented in this study provide a surface comparison of SMIL coatings applying 55% PAMAMPS or DS as terminal layer and show their influence on the EOF and the CZE separation of closely related proteins. Thereby, the charge density of 55% PAMAMPS is lower than for DS (Fig. 1B, A). The behavior of 55% PAMAMPS in the outlined SMIL coating in CZE separations of proteins will be comprehensively described in another publication.

Measuring morphology and charge distribution on the inner wall of a SMIL coated capillary used for CZE requires the following steps. (1) Functionalization of the capillary. (2) Fast and gentle preparation protocol to allow direct contact of the adhesion sensing tip (3) to the inner capillary surface. (4) Test of the sensing molecule to ensure sufficient interactions. Finally, (5) the surface has to be scanned laterally using an upgraded sensing device yielding morphology and adhesion map with nanometer resolution.

3.1. Comparison of CZE performance of SMIL coated capillaries with different terminal layer

The CZE performance of different SMIL-capillaries is demonstrated in Fig. 1D, E. Therefore, circular capillaries with 4-layer SMIL coatings with 55% PAMAMPS or DS as terminal layer were compared. A recombinant isoform of the pollen allergen of birch (*Betula verrucosa*), i.e. Bet v 1a, was in-lab nitrated with peroxynitrite and used as a model system. Nitration occurs at tyrosine residues and slightly reduces the isoelectric points of resulting nitration variants [47]. Depending on the position of the induced modification, even Bet v 1a variants of identical nitration grade could be separated [42]. Thus, nitrated Bet v 1a was selected as an appropriate model sample. The μ_{EOF} in the SMIL-coated circular capillary with 55% PAMAMPS was 3.90×10^{-4} $cm^2.V^{-1}.s^{-1}$, whereas the SMIL coating with terminal DS provided an μ_{EOF} of 4.46×10^{-4} $cm^2.V^{-1}.s^{-1}$ under the selected separation conditions (Fig. 1D, E). Thus, the μ_{EOF} became reduced by ~13% when using 55% PAMAMPS as terminal SMIL layer. This is consistent with the reduced charge density of the applied terminal layer, i.e. 55% PAMAMPS in comparison to DS. Due to its lower μ_{EOF} the SMIL coating with 55% PAMAMPS (showed an improved resolution of minor nitration variants when analyzing the same allergen batch (Fig. 1D, E with inserts)).

3.2. Capillary preparation for AFM measurements

AFM investigation of the inner part of an electrophoresis capillary is challenging due to its small dimensions and accessibility with the AFM tip. Consistently, we investigated rectangular shaped capillaries (Fig. 2A) which allow an easier AFM investigation. Thus optimized mounting and opening protocols were developed performing all steps under buffered conditions and avoiding artefacts as known to appear using smashing or grinding [24]. We tested two different approaches for mechanical opening, both optimized for square shaped capillaries. First, we performed a cut rectangular to the capillary axis as shown in Fig. 2B. Although the cutting itself can be done easily and quick, the positioning of the AFM cantilever remains challenging. It is very critical that the orientation of the cantilever is perfectly aligned with the axis of the capillary. Alternatively, we applied a second optimized cutting method. By applying gentle force to the side section of the broken capillary we were able to cut the capillary (partly) along its axis. Although this opening procedure is more challenging, it allows easier positioning of the cantilever. The latter was realized by

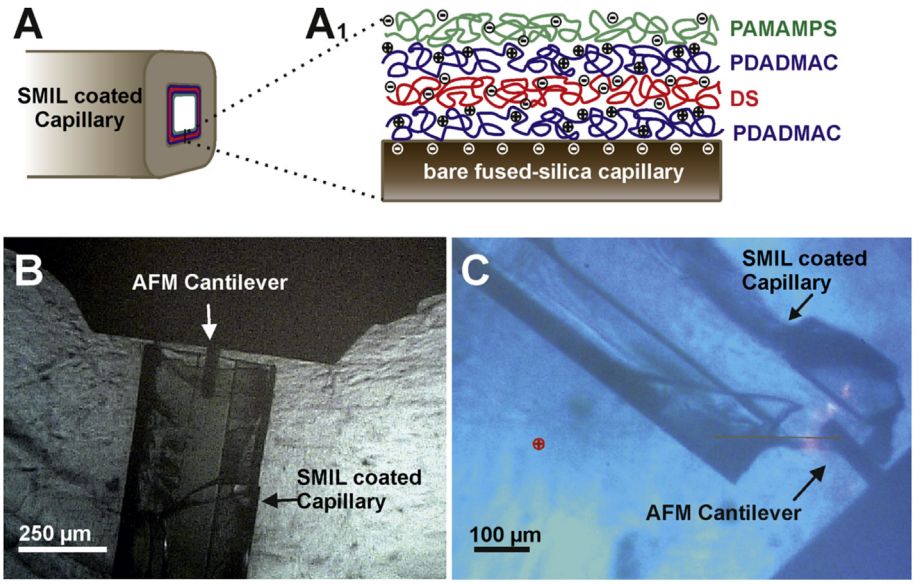

Fig. 2. (A) Square capillary with SMIL coating. (A_1) Insert provides a detailed SMIL stratification. (B) An AFM cantilever is positioned in the freshly opened inner capillary tube in aligned orientation by moving it into the hole of a vertically cut capillary. (C) If the capillary is cut in axial direction the cantilever has to be adjusted above the opened area.

adjusting the cantilever exactly above the (accessible) area of capillary (Fig. 2C) followed by simple approaching of the cantilever to the capillary surface. Both presented methods allow fast, glass splinter and artefact-free AFM imaging and sensing investigations which are offering an optimal basis for biosensing AFM measurements.

3.3. AFM tip chemistry

Both applied AFM biosensing techniques, MRFS and TREC, rely on the upgrade of tips using specific biomolecules. Thus, the same functionalization scheme can be applied. To mimic a realistic situation for charge sensing we decided to use the positively charged protein avidin for sensing of negatively charged coatings. Avidin, a very stable and robust mid-sized protein is known to have a high isoelectric point (~10.5) and thus is highly positively charged at neutral pH [48]. The anchoring of avidin was performed following a well-established protocol for tip functionalization [39,43,49] as shown in Fig. 3A including (1) aminofunctionalization, (2) binding of a heterobifunctional linker, and (3) the sensing protein (avidin or streptavidin). PEG used as linker material brings thereby the advantage of its stretchability which is a prerequisite for both, MRFS and TREC, but also acts as non-adherent chemical avoiding interactions caused by other molecules than the sensing molecule.

3.4. Molecular recognition force spectroscopy

MRFS is an innovative tool to investigate adhesion forces at the single molecule level [50–52] which has been applied to explore the energy landscape of isolated proteins, artificial and native biomembranes as well as different types of fixed and living cells (for review see Ref. [52]). In our study, MRFS experiments were applied as proof of principle to ensure charge induced binding of the sensing molecule at inversely charged surfaces (i.e. PDADMAC-DS-PDADMAC-55% PAMAMPS and PDADMAC-DS-PDADMAC-DS) and to quantify this interaction strength. Furthermore MRFS was performed to gain insights into the adhesive interactions of all intermediate formed layers ranging from PDADMAC over PDADMAC-DS, to PDADMAC-DS-PDADMAC. Since we were interested to investigate the distributions of negative charges, i.e. SMIL surface coverage by the terminal 55% PAMAMPS or DS layer, we used the positively charged avidin molecule as sensor. Thus, freshly prepared avidin functionalized tips were used immediately after preparation. As a test surface a square shaped fused-silica capillary with a SMIL coating on its outside was prepared and tested (see Sections 2.2 and 2.6). Due to the negative charge of 55% PAMAMPS or DS an electrostatic interaction was expected. To measure the adhesion forces, the avidin functionalized tip was repeatedly approached to – and withdrawn from – the different SMIL coated surface. In all cases, the indentation force was limited to ~400 pN to ensure nondestructive measurements. While being in direct physical contact, the avidin molecule has the ability to adhere to the SMIL coatings as a result of expected mainly electrostatic attractions. As exemplary shown for the PDADMAC-DS-PDADMAC-55% PAMAMPS – avidin interaction in Fig. 3B, only an upwards bending of the cantilever can be observed in the approaching period (Fig. 3B red line), whereas the retraction curve exhibits a second, but this time downwards, bending after losing contact (Fig. 3B black line, highlighted with an arrow). This gives a clear evidence of adherence. To statistically verify this, 1500–2000 FDCs were performed. As a result we could show that adherence appeared with a binding probability (BP) of 22.3 ± 6% (Fig. 3C, blue line), for the PDADMAC-DS-PDADMAC-55% PAMAMPS – avidin and 22.5 ± 5% for the PDADMAC-DS-PDADMAC-DS – avidin interaction thus reflecting a probability of interaction close to the upper limit [53] when using PEG based chemistry in both cases. The most probable unbinding force was 56.7 ± 13 pN at a most probable unbinding length of 16.8 ± 3 nm (n = 4) for 55% PAMAMPS and 60.0 ± 10 pN at a most probable unbinding length of 12.9 ± 4 nm (n = 4) for DS as final layer. To further prove the electrostatic nature of this interaction we performed force spectroscopy experiments on the very same SMIL surface (PDADMAC-DS-PDADMAC-55% PAMAMPS) using the similar but neutral charged protein streptavidin. Here the binding probability dropped down significantly to 1.5 ± 0.5%, whereas no pronounced unbinding length and force was observed (Fig. 3C, green line). To determine possible influences of the tip functionalization except the (avidin or streptavidin) protein itself, a PEG functionalized tip without any coupled protein was

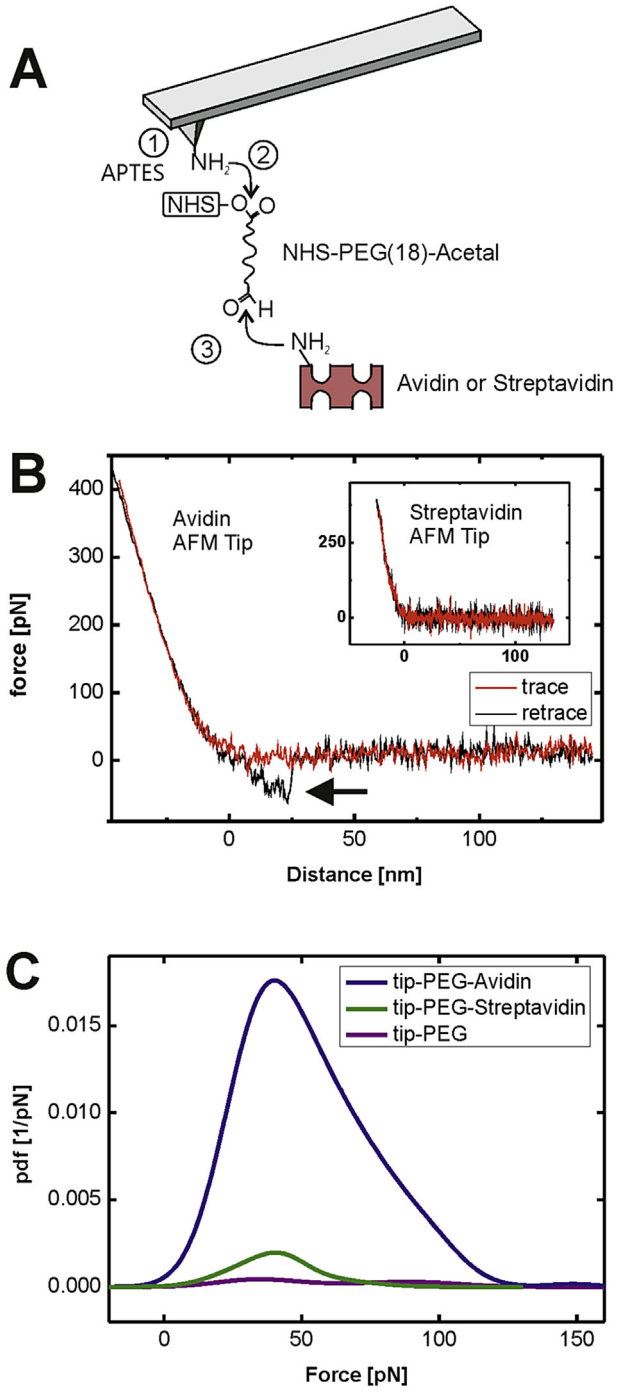

Fig. 3. Molecular Recognition Force Spectroscopy. (A) Tip chemistry: An APTES coated tip (1) is functionalized with a heterobifunctional NHS-PEG(18)-Acetal crosslinker (2) via amide formation. The deprotected acetal residue of the linker is used to tether the adhesion sensor molecule avidin (or streptavidin) to the tip (3). (B) Typical force distance cycle showing interaction of the positively charged (tip bound) avidin with a (negatively charged) outer SMIL layer (55% PAMAMPS). In contrast, an (uncharged) streptavidin functionalized tip does not show any interaction with the same layer. (C) Probability density functions (pdf) of the interactions of 55% PAMAMPS surfaces with avidin (blue line), streptavidin (green line), and protein-free tips (purple line). The probability of molecular electrostatic adhesion events drops from 22.3 ± 6% for avidin to 1.5 ± 0.5% for streptavidin and 0.6 ± 0.3% for protein-free tips. The curves are normalized to their relative binding probability. (For interpretation of the references to colour in this figure legend, the reader is referred to the web version of this article.)

used for MRFS at the same surface and showed again nearly no interaction (Fig. 3C, purple line) with a binding probability of 0.6 ± 0.3%. Summarizing, we could clearly demonstrate the usability of PEG tethered avidin functionalized AFM tips as electrostatic sensors fulfilling the requirements for recognition imaging.

In addition, we compared the adhesive properties of simpler coatings, namely of the stepwise formed layers ranging from PDADMAC, PDADMAC-DS, PDADMAC-DS-PDADMAC to PDADMAC-DS- PDADMAC-DS. As expected no interaction was determined on the first (2.3 ± 3.2% BP) and third layer (5.3 ± 4.6% BP), namely PDADMAC, whereas the second layer (i.e. the first DS layer) yielded very comparable results to the final layer (56.8 ± 6 pN rupture force with a BP of 22.5 ± 5%, n = 4).

3.5. TREC measurements

Topography and recognition imaging is based on the use of biosensing AFM tips and allows simultaneous measurement of sample topography and recognition map without loss in lateral resolution and imaging speed compared to conventional tapping mode [33,54–56]. TREC has successfully been applied to map for recognition sites of isolated proteins [33,54], on artificial [35] and native biomembranes [36], and whole cells [57–59]. Here we utilized the electrostatic interaction of the positively charged avidin molecule to map the adhesion sites of the negatively charged outer SMIL layers (55% PAMAMPS and DS). From the previously performed MRFS experiments based on the very same tip functionalization and capillary coating protocols, the acting electrostatic forces were known, 56.7 ± 13 pN for avidin – 55% PAMAMPS and 60.0 ± 10 pN for avidin – DS (final layer), no interaction was observable for streptavidin – 55% PAMAMPS (or PEG – 55% PAMAMPS). We now applied TREC mode AFM imaging on the inner capillary surface of different freshly prepared SMIL coated capillaries as shown in Fig. 4A (55% PAMAMPS) and Fig. 4C (DS). The topography of the terminal 55% PAMAMPS layer appeared rather flat with a RMS roughness of 1.43 ± 0.07 nm (n = 3) and only slightly increased to 1.56 ± 0.08 nm (n = 3) after the NaOH rinsing of the very same capillary. A slightly higher surface roughness was measured on the terminal DS layer (roughness of 2.1 ± 0.2 nm, n = 3.). In contrast, for the 55% PAMAMPS layer, the homogeneously distributed adhesion (red and yellow areas in Fig. 4A, lower image) dramatically changed after the NaOH treatment. As shown in Fig. 4B (lower image) the surface appeared more heterogeneous. In addition to areas with high adhesion (red-yellow) also areas without or with low adhesion (green) appeared. Thus, it is evident that the adhesive properties got altered by the NaOH treatment. Interestingly, if one looks at the average distance between two peaks on the topographical trace for PDADMAC-DS-PDADMAC-55% PAMAMPS coating, which is about 38 nm (13 inter peak distances on the whole 500 nm range), it is close to the hydrodynamic diameter (or typical size) of the 55% PAMAMPS chain which was determined to be 40–42 nm by Taylor dispersion analysis in the storage buffer. Therefore, each 'cloudy' white spot (on topography pictures) or red spot (on adhesion pictures) may be interpreted as the top of an adsorbed 55% PAMAMPS chain. For PDADMAC-DS-PDADMAC-DS coating, the inter peak distances increased in good agreement with the higher hydrodynamic diameter of DS (~90–100 nm). In an ongoing study (manuscript in progress) the analytical performance of such a SMIL coated capillary at different stages of their coating is cross correlated with their topographical appearance and its adhesive behavior. The comparison of PDADMAC-DS-PDADMAC-55% PAMAMPS with PDADMAC-DS-PDADMAC-DS layer show clear differences in both, surface roughness (Fig. 4A and C, upper images) which can be explained by the branched structure of DS (Fig. 1A), but also in their lateral distribution of charges (Fig. 4A and C, lower images).

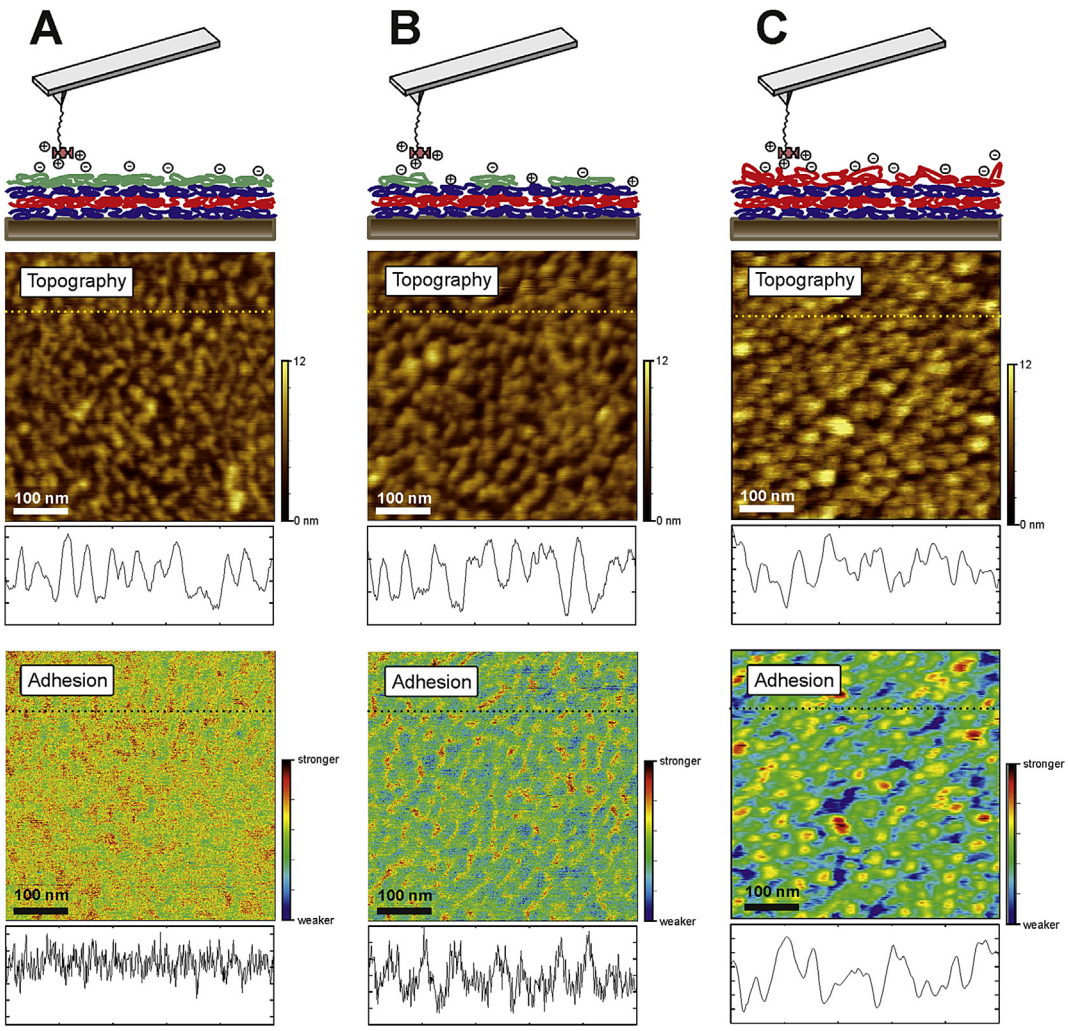

Fig. 4. Molecular adhesion measurements of PDADMAC-DS-PDADMAC-55% PAMAMPS SMIL coated capillaries before (A) and after (B) NaOH treatment and (C) PDADMAC-DS-PDADMAC-DS SMIL coated capillary. Freshly prepared SMIL capillaries were imaged using an avidin functionalized tip (A, top) resulting in a smooth surface showing protrusions of 1–5 nm (A, middle) and an rms roughness of 1.43 nm. In contrast, the adhesion image reveals a rather homogenously distributed adhesion (A, bottom). Although the surface topography of NaOH treated SMIL coated capillaries (B, top) show only minor changes in their surface topography (B, middle) (rms roughness of 1.56 nm) the adhesion map (B, bottom) appears significantly more heterogeneous. Surfaces with a final DS layer (C, top) showed increased size of polymers (c, middle) and more heterogeneous adhesion properties (c, bottom) compared to 55% PAMAMPS as final layer. Z-range for the adhesion images is set to 50 mV. The scaling for the cross-section of the topographical images is 9 nm and for the adhesion images 60 mV.

4. Discussion and conclusions

Capillary electrophoresis is an essential analytical tool with prosperous future perspectives in the characterization of intact proteins. Coating of the inner surface of separation capillaries thereby allows for a further improvement of CZE performance. SMIL coatings experience increasing interest and application due to their straightforward preparation with consistent performance. However, the characterization of the inner capillary surface is still an obstacle in the purposive optimization of capillary coatings and their treatments. Particularly, elucidation of molecular processes that happen at the surface of coatings while it degrades and the separation impairs but also during remedying strategies, i.e. rinsing and refreshment of coatings, are required which demands related tools for quality control and characterization. AFM, beside electron microscopy and XPS (which both do not allow measurements under buffered conditions mimicking the real situation), offers a powerful tool for investigation of such coatings at the nanoscale. In contrast to the excellent AFM imaging studies of other groups, we developed for the first time a direct functional investigation approach yielding in parallel information about the morphology and the adhesive properties of the coating of the inner capillary wall which is indispensable for understanding adsorptive effects. Furthermore, we determined the electrostatic interaction forces between an opposed charged protein (tethered on a sharp cantilever tip) and the capillary surface at different coatings and different stages of preparation. To demonstrate the ability to monitor adhesive changes at the nanoscale we compared two different states of the coating. TREC adhesion imaging clearly resolved significant differences in the ability of charge induced adhesion which cannot be followed by simple topographical imaging, since morphological changes do not reflect functional variations in sufficient manner. In addition, we could determine clear differences of the charge distributions of PDADMAC-DS-PDADMAC-55% PAMAMPS and PDADMAC-DS-PDADMAC-DS coated capillaries which show a comparable interaction force towards positively charged avidin molecules. We believe that recognition imaging offers a promising tool for functional investigations of

electrophoresis capillaries and thus closing a knowledge gap needed for a more in-depth understanding in this field.

Acknowledgements

We are grateful to Dr. Christian Rankl for providing his Matlab based semi-automatic data evaluation program *kspec19*. MSc Sergey Gusenkov is kindly acknowledged for preparing and providing nitrated Bet v 1a. The financial support by the Austrian Federal Ministry of Science, Research, and Economy and by a Start-up Grant of the State of Salzburg is gratefully acknowledged.

References

[1] K. Salomon, D.S. Burgi, J.C. Helmer, Evaluation of fundamental properties of a silica capillary used for capillary electrophoresis, J. Chromatogr. A 559 (1) (1991) 69–80.
[2] H. Stutz, G. Bordin, A.R. Rodriguez, Separation of selected metal-binding proteins with capillary zone electrophoresis, Anal. Chim. Acta 477 (1) (2003) 1–19.
[3] H. Stutz, Protein attachment onto silica surfaces–a survey of molecular fundamentals, resulting effects and novel preventive strategies in CE, Electrophoresis 30 (12) (2009) 2032–2061.
[4] E.A. Doherty, et al., Microchannel wall coatings for protein separations by capillary and chip electrophoresis, Electrophoresis 24 (1–2) (2003) 34–54.
[5] B. Verzola, C. Gelfi, P.G. Righetti, Protein adsorption to the bare silica wall in capillary electrophoresis: quantitative study on the chemical composition of the background electrolyte for minimising the phenomenon, J. Chromatogr. A 868 (1) (2000) 85–99.
[6] M. Punzet, et al., Profiling preparations of recombinant birch pollen allergen Bet v 1a with capillary zone electrophoresis in pentamine modified fused-silica capillaries, J. Chromatogr. B 839 (1) (2006) 19–29.
[7] B. Kronsteiner, H. Malissa, H. Stutz, Profiling recombinant major birch pollen allergen Bet v 1a and carbamylated variants with CZE and CIEF, Electrophoresis 28 (13) (2007) 2241–2251.
[8] L. Pei, C.A. Lucy, Insight into the stability of poly (diallydimethylammonium-chloride) and polybrene poly cationic coatings in capillary electrophoresis, J. Chromatogr. A 1365 (2014) 226–233.
[9] S. Bekri, L. Leclercq, H. Cottet, Polyelectrolyte multilayer coatings for the separation of proteins by capillary electrophoresis: influence of polyelectrolyte nature and multilayer crosslinking, J. Chromatogr. A 1399 (2015) 80–87.
[10] C.A. Lucy, A.M. MacDonald, M.D. Gulcev, Non-covalent capillary coatings for protein separations in capillary electrophoresis, J. Chromatogr. A 1184 (1) (2008) 81–105.
[11] J. Horvath, V. Dolnik, Polymer wall coatings for capillary electrophoresis, Electrophoresis 22 (4) (2001) 644–655.
[12] M. Weinbauer, H. Stutz, Successive multiple ionic polymer layer coated capillaries in the separation of proteins–recombinant allergen variants as a case study, Electrophoresis 31 (11) (2010) 1805–1812.
[13] M. Hamer, A. Yone, I. Rezzano, Gold nanoparticle-coated capillaries for protein and peptide analysis on open-tubular capillary electrochromatography, Electrophoresis 33 (2) (2012) 334–339.
[14] Y. He, et al., Capillary modified with covalently attached coating for enhanced CE separation of biopolymers, Electrophoresis 31 (4) (2010) 630–633.
[15] H. Katayama, Y. Ishihama, N. Asakawa, Stable cationic capillary coating with successive multiple ionic polymer layers for capillary electrophoresis, Anal. Chem. 70 (24) (1998) 5272–5277.
[16] H. Katayama, Y. Ishihama, N. Asakawa, Stable capillary coating with successive multiple ionic polymer layers, Anal. Chem. 70 (11) (1998) 2254–2260.
[17] Y. Liu, et al., Dynamic coating using polyelectrolyte multilayers for chemical control of electroosmotic flow in capillary electrophoresis microchips, Anal. Chem. 72 (24) (2000) 5939–5944.
[18] R. Nehmé, et al., Influence of polyelectrolyte coating conditions on capillary coating stability and separation efficiency in capillary electrophoresis, Electrophoresis 29 (14) (2008) 3013–3023.
[19] J.R. Catai, et al., Analysis of recombinant human growth hormone by capillary electrophoresis with bilayer-coated capillaries using UV and MS detection, J. Chromatogr. B 852 (1) (2007) 160–166.
[20] T.W. Graul, J.B. Schlenoff, Capillaries modified by polyelectrolyte multilayers for electrophoretic separations, Anal. Chem. 71 (18) (1999) 4007–4013.
[21] R. Haselberg, G.J. De Jong, G.W. Somsen, Capillary electrophoresis–mass spectrometry of intact basic proteins using polybrene–dextran sulfate–polybrene-coated capillaries: system optimization and performance, Anal. Chim. Acta 678 (1) (2010) 128–134.
[22] J.R. Catai, G.W. Somsen, G.J. de Jong, Efficient and reproducible analysis of peptides by capillary electrophoresis using noncovalently bilayer-coated capillaries, Electrophoresis 25 (6) (2004) 817–824.
[23] S. Amon, A. Plematl, A. Rizzi, Capillary zone electrophoresis of glycopeptides under controlled electroosmotic flow conditions coupled to electrospray and matrix-assisted laser desorption/ionization mass spectrometry, Electrophoresis 27 (5–6) (2006) 1209–1219.
[24] H. Wätzig, S. Kaupp, M. Graf, Inner surface properties of capillaries for electrophoresis, TrAC Trends Anal. Chem. 22 (9) (2003) 588–604.
[25] S. Kaupp, H. Wätzig, Characterization of inner surface phenomena in capillary electrophoresis capillaries by electron microscopy, atomic force microscopy and secondary ion mass spectroscopy, J. Chromatogr. A 781 (1) (1997) 55–65.
[26] J.J. Bonvent, et al., Adsorption of proteins to fused-silica capillaries as probed by atomic force microscopy, J. Chromatogr. A 756 (1) (1996) 233–243.
[27] A. Cifuentes, et al., Polyacrylamide-coated capillaries probed by atomic force microscopy: correlation between surface topography and electrophoretic performance, Anal. Chem. 70 (16) (1998) 3458–3462.
[28] E. Mansfield, E.E. Ross, C.A. Aspinwall, Preparation and characterization of cross-linked phospholipid bilayer capillary coatings for protein separations, Anal. Chem. 79 (8) (2007) 3135–3141.
[29] R. Haselberg, et al., Thickness and morphology of polyelectrolyte coatings on silica surfaces before and after protein exposure studied by atomic force microscopy, Anal. Chim. Acta 779 (2013) 90–95.
[30] L. Moore Jr., et al., Lysine-based zwitterionic molecular micelle for simultaneous separation of acidic and basic proteins using open tubular capillary electrochromatography, Anal. Chem. 82 (10) (2010) 3997–4005.
[31] R. Barberi, et al., Probing soft polymeric coatings of a capillary by atomic force microscopy, J. Chromatogr. B Biomed. Sci. Appl. 683 (1) (1996) 3–13.
[32] N.E. Baryla, et al., Characterization of surfactant coatings in capillary electrophoresis by atomic force microscopy, Anal. Chem. 73 (19) (2001) 4558–4565.
[33] A. Ebner, et al., Localization of single avidin-biotin interactions using simultaneous topography and molecular recognition imaging, Chemphyschem 6 (5) (2005) 897–900.
[34] M. Leitner, et al., Single-molecule AFM characterization of individual chemically tagged DNA tetrahedra, Acs Nano 5 (9) (2011) 7048–7054.
[35] J. Tang, et al., Recognition imaging and highly ordered molecular templating of bacterial S-Layer nanoarrays containing affinity-tags, Nano Lett. 8 (12) (2008) 4312–4319.
[36] A. Ebner, et al., Determination of CFTR densities in erythrocyte plasma membranes using recognition imaging, Nanotechnology 19 (38) (2008), 384017, 6.
[37] L. Chtcheglova, et al., Development of recognition imaging: from molecules to cells, Atomic Force Microsc. Nanobiol. (2014) 111–142.
[38] S. Senapati, S. Lindsay, Recent progress in molecular recognition imaging using atomic force microscopy, Acc. Chem. Res. 49 (3) (2016) 503–510.
[39] L. Wildling, et al., Linking of sensor molecules with amino groups to amino-functionalized AFM tips, Bioconjug. Chem. 22 (6) (2011) 1239–1248.
[40] G. Danger, M. Ramonda, H. Cottet, Control of the EOF in CE using polyelectrolytes of different charge densities, Electrophoresis 28 (6) (2007) 925–931.
[41] J. Chamieh, H. Cottet, Comparison of single and double detection points Taylor dispersion analysis for monodisperse and polydisperse samples, J. Chromatogr. A 1241 (2012) 123–127.
[42] S. Gusenkov, C. Ackaert, H. Stutz, Separation and characterization of nitrated variants of the major birch pollen allergen by CZE-ESI-μTOF MS, Electrophoresis 34 (18) (2013) 2695–2704.
[43] A. Ebner, et al., Functionalization of probe tips and supports for single-molecule recognition force microscopy, Top. Curr. Chem. 285 (2008) 29–76 (Stm and Afm Studies on (Bio)Molecular Systems: Unravelling the Nanoworld).
[44] A. Ebner, P. Hinterdorfer, H.J. Gruber, Comparison of different amino-functionalization strategies for attachment of single antibodies to AFM cantilevers, Ultramicroscopy 107 (10–11) (2007) 922–927.
[45] H.-J. Butt, M. Jaschke, Calculation of thermal noise in atomic force microscopy, Nanotechnology 6 (1) (1995) 1.
[46] W. Baumgartner, P. Hinterdorfer, H. Schindler, Data analysis of interaction forces measured with the atomic force microscope, Ultramicroscopy 82 (1) (2000) 85–95.
[47] B. Alvarez, R. Radi, Peroxynitrite reactivity with amino acids and proteins, Amino Acids 25 (3–4) (2003) 295–311.
[48] O. Livnah, et al., Three-dimensional structures of avidin and the avidin-biotin complex, Proc. Natl. Acad. Sci. 90 (11) (1993) 5076–5080.
[49] A. Ebner, et al., A new, simple method for linking of antibodies to atomic force microscopy tips, Bioconjug. Chem. 18 (4) (2007) 1176–1184.
[50] E.-L. Florin, V.T. Moy, H.E. Gaub, Adhesion forces between individual ligand-receptor pairs, Science 264 (5157) (1994) 415–417.
[51] E. Evans, K. Ritchie, Dynamic strength of molecular adhesion bonds, Biophys. J. 72 (4) (1997) 1541–1555.
[52] A. Ebner, et al., Probing the energy landscape of protein-binding reactions by dynamic force spectroscopy, in: P. Hinterdorfer, A. Oijen (Eds.), Handbook of Single-Molecule Biophysics, Springer, New York, 2009, pp. 407–447.
[53] A. Ebner, et al., Single molecule force microscopy on cells and biological membranes, Curr. Nanosci. 3 (1) (2007) 49–56.
[54] C. Stroh, et al., Single-molecule recognition imaging microscopy, Proc. Natl. Acad. Sci. U. S. A. 101 (34) (2004) 12503–12507.
[55] J. Preiner, et al., Simultaneous topography and recognition imaging: physical aspects and optimal imaging conditions, Nanotechnology 20 (21) (2009) 215103.
[56] F. Kienberger, et al., Molecular recognition imaging and force spectroscopy of single biomolecules, Acc. Chem. Res. 39 (1) (2006) 29–36.

[57] L.A. Chtcheglova, et al., Localization of the ergtoxin-1 receptors on the voltage sensing domain of hERG K+ channel by AFM recognition imaging, Pflugers Arch. Eur. J. Physiol. 456 (1) (2008) 247–254.
[58] M. Zhang, et al., Mapping out the structural changes of natural and pretreated plant cell wall surfaces by atomic force microscopy single molecular recognition imaging, Biotechnol. Biofuels 6 (1) (2013) 147, 11.
[59] W. Zhao, et al., Detection of carbohydrates on the surface of cancer and normal cells by topography and recognition imaging, Chem. Commun. 49 (29) (2013) 2980–2982.